Leptospiral lipopolysaccharide dampens inflammation through upregulation of autophagy adaptor p62 and NRF2 signaling in macrophages

Delphine Bonhomme, Ignacio Santecchia, Pedro Escoll, Stylianos Papadopoulos, Frédérique Vernel-Pauillac, Ivo G Boneca, Catherine Werts

▶ **To cite this version:**

Delphine Bonhomme, Ignacio Santecchia, Pedro Escoll, Stylianos Papadopoulos, Frédérique Vernel-Pauillac, et al.. Leptospiral lipopolysaccharide dampens inflammation through upregulation of autophagy adaptor p62 and NRF2 signaling in macrophages. Microbes and Infection, 2024, 26 (3), pp.105274. 10.1016/j.micinf.2023.105274 . pasteur-04600407

HAL Id: pasteur-04600407
https://pasteur.hal.science/pasteur-04600407v1

Submitted on 4 Jun 2024

HAL is a multi-disciplinary open access archive for the deposit and dissemination of scientific research documents, whether they are published or not. The documents may come from teaching and research institutions in France or abroad, or from public or private research centers.

L'archive ouverte pluridisciplinaire **HAL**, est destinée au dépôt et à la diffusion de documents scientifiques de niveau recherche, publiés ou non, émanant des établissements d'enseignement et de recherche français ou étrangers, des laboratoires publics ou privés.

Distributed under a Creative Commons Attribution - NonCommercial - NoDerivatives 4.0 International License

Microbes and Infection 26 (2024) 105274

Contents lists available at ScienceDirect

Microbes and Infection

journal homepage: www.elsevier.com/locate/micinf

Original article

Leptospiral lipopolysaccharide dampens inflammation through upregulation of autophagy adaptor p62 and NRF2 signaling in macrophages

Delphine Bonhomme [a], Ignacio Santecchia [a], Pedro Escoll [b], Stylianos Papadopoulos [a], Frédérique Vernel-Pauillac [a], Ivo G. Boneca [a], Catherine Werts [a, *]

[a] Institut Pasteur, Université Paris Cité, CNRS UMR6047, INSERM U1306, Unité de Biologie et Génétique de la Paroi Bactérienne, Paris, France
[b] Institut Pasteur, Université Paris Cité, CNRS UMR6047, Unité Biologie des Bactéries Intracellulaires, Paris, France

ARTICLE INFO

Article history:
Received 11 May 2023
Accepted 6 December 2023
Available online 9 December 2023

Keywords:
Leptospira
LPS
TLRs
Autophagy adapter p62
NRF2

ABSTRACT

Leptospira interrogans are pathogenic bacteria responsible for leptospirosis, a worldwide zoonosis. All vertebrates can be infected, and some species like humans are susceptible to the disease whereas rodents such as mice are resistant and become asymptomatic renal carriers. Leptospires are stealth bacteria that are known to escape several immune recognition pathways and resist killing mechanisms. We recently published that leptospires may survive intracellularly in and exit macrophages, avoiding xenophagy, a pathogen-targeting form of autophagy. Interestingly, the latter is one of the antimicrobial mechanisms often highjacked by bacteria to evade the host immune response. In this study we explored whether leptospires subvert the key molecular players of autophagy to facilitate infection. We showed in macrophages that leptospires triggered a specific accumulation of autophagy-adaptor p62 in puncta-like structures, without altering autophagic flux. We demonstrated that *Leptospira*-induced p62 accumulation is a passive mechanism depending on the leptospiral virulence factor LPS signaling via TLR4/TLR2. p62 is a central pleiotropic protein, also mediating cell stress and death, *via* the translocation of transcription factors. We demonstrated that *Leptospira*-driven accumulation of p62 induced the translocation of transcription factor NRF2, a key player in the anti-oxidant response. However, NRF2 translocation upon *Leptospira* infection did not result as expected in antioxydant response, but dampened the production of inflammatory mediators such as iNOS/NO, TNF and IL6. Overall, these findings highlight a novel passive bacterial mechanism linked to LPS and p62/NRF2 signaling that decreases inflammation and contributes to the stealthiness of leptospires.

© 2023 The Author(s). Published by Elsevier Masson SAS on behalf of Institut Pasteur. This is an open access article under the CC BY-NC-ND license (http://creativecommons.org/licenses/by-nc-nd/4.0/).

Leptospira interrogans are spirochete bacteria and the causative agent of leptospirosis, a neglected worldwide zoonosis whose global impact on human health is increased due to climate change, and causes around 60 000 deaths *per* year worldwide [1]. Although all vertebrates can be infected by leptospires, they do not all present the same symptoms and susceptibility to the disease [2]. Humans, as sensitive hosts, may suffer from acute leptospirosis ranging from flu-like symptoms to multi-organ failure in 5–10 % cases [1]. On the other hand, rodents such as mice and rats are resistant to acute illness and become chronically colonized upon infection [3]. Leptospires establish a stable colonization in the proximal tubules in the kidneys, that leads to their excretion in the urine throughout the life of the animal, contributing to the spread of the zoonosis [3,4].

Upon infection, the host immune defenses rely on humoral and cellular components, such as the complement system, immunoglobulins, and phagocytes. Activation of immune cells such as macrophages is mediated by the sensing of microbial associated molecular patterns (MAMPs) by pattern recognition receptors (PRRs). Leptospires are agonists of TLR2, through their numerous lipoproteins [5,6], and activate the NLRP3 inflammasome [7]. However, they are remarkable as stealth pathogens that escape recognition by NOD receptors [8] and by TLR5 [9] through unique mechanisms. Furthermore, the leptospiral lipopolysaccharide (LPS), a central virulence factor [10], possesses structural peculiarities [11] that do not activate human TLR4 [12], whereas they partially

* Corresponding author. Institut Pasteur, 28 rue du Dr Roux, Unité BGPB, Microbiology Dpt, Paris 75015 France.
E-mail address: cwerts@pasteur.fr (C. Werts).

https://doi.org/10.1016/j.micinf.2023.105274
1286-4579/© 2023 The Author(s). Published by Elsevier Masson SAS on behalf of Institut Pasteur. This is an open access article under the CC BY-NC-ND license (http://creativecommons.org/licenses/by-nc-nd/4.0/).

activate murine TLR4 [13]. In addition to escaping PRR recognition, leptospires also escape some phagocytic functions. Although leptospires are mostly extracellular bacteria, we previously reported that they can be found within macrophages without intracellular replication [14], and are neither targeted by phagocytosis nor classical microbicidal compounds [14]. We further excluded that intracellular leptospires could be targeted by xenophagy [14], a specific form of autophagy promoting the degradation of intracellular pathogens [15–17].

Interestingly, among the numerous proteins involved in autophagy, many have pleiotropic roles that are not restricted to autophagic-degradation and are at the crossroads between autophagy, cell death, cellular stress and inflammation. For instance, autophagy adaptors p62 and NDP52, which traditionally bridge the cargo and autophagosome for specific degradation, have been associated with many xenophagy-independent inflammatory modulations [18,19]. Both p62 and NDP52 have been shown to mediate nuclear translocation of transcription factors NFκB and NRF2, which are involved in inflammation and cellular stress, respectively [18,20].

In this study, we focused our investigations on autophagy adaptors and interestingly found in macrophages infected with leptospires that their LPS dampened inflammation by modulating the p62/NRF2 axis.

1. Materials and methods

1.1. L. interrogans *cultures*

L. interrogans used (Manilae strain L495, Copenhageni strain Fiocruz L1-130, Icterohaemorragiae strain Verdun) and *Leptospira biflexa* (Patoc strain Patoc I) were grown in Ellinghausen-McCullough-Johnson-Harris (EMJH) medium at 28 °C without agitation and diluted weekly (twice a week for *L. biflexa*) to obtain exponential cultures. For infection, cultures were centrifuged (3250 g, 25 min), resuspended in PBS (Lonza), and enumerated in Petroff-Hauser chamber. Inactivated leptospires ("heat-killed") were heated at 56 °C for 30 min with mild agitation. For fluorescent labelling, 10 mL of exponential culture was centrifuged (3250 g, 25 min) and the pellet was resuspended in the same volume of PBS (Lonza) with addition of 10 μM CFSE (Sigma) for 30 min, followed by one wash in PBS before counting and infection.

1.2. Mice experiments

Adults male and female C57/BL6J mice (Janvier Labs, Le Genest-Saint-Isle, France) were injected *via* intraperitoneal route with 1×10^8 heat-killed leptospires/mouse in PBS. Next, 4h post-infection mice were euthanized, and peritoneal content was recovered as previously described [21]. Peritoneal cells were plated at 1×10^6 cells/mL and were let to adhere for 1h before fixation and immunofluorescence staining.

1.3. Cell culture

Bone marrow derived macrophages (BMDMs) were obtained and derived from adults male and female mice of either C57BL/6J WT (Janvier Labs, Le Genest-Saint-Isle, France) or TLR2$^{-/-}$ TLR4$^{-/-}$, and double TLR2$^{-/-}$ TLR4$^{-/-}$ (dko) (from Institut Pasteur) as described before [13]. BMDMs were seeded in plates (TPP) the day before infection at a concentration of 0.8×10^6 cells/mL, in antibiotic-free complete RPMI (RPMIc) (containing glutamine (Lonza), supplemented with 10 % v/v heat-inactivated fetal calf serum (HI-FCS, Gibco), 1 mM non-essential amino acids (NEA, Gibco) and 1 mM sodium pyruvate (NaPy, Gibco)).

RAW264.7 and RAW-ASC murine macrophage-like cell line was cultured in antibiotic-free RPMIc. RAW-mLC3-DiFluo (Invivogen) autophagy reporter cells (transfected with LC3-GFP-RFD) were cultured with 100 μg/mL zeocin (Invivogen). Cells were seeded in plates (TPP) the day before infection at a concentration of 0.3×10^6 cells/mL, in antibiotic-free RPMIc.

Human THP-1 monocyte-like cell line, stably transfected with CD14 (THP1-CD14), was cultured in RPMIc and seeded at 1×10^6 cells/mL.

All cell cultures were tested negative for *Mycoplasma* contamination, and all cell cultures used for experiments were maintained under 80 % confluence in order to prevent autophagic stress.

Cell starvation was induced in EBSS media (Gibco) after 2 washes. Autophagy blockage was induced with 100 nM bafilomycin A1 (BafA1, Sigma–Aldrich) 4h before cell collection. Inflammasome inhibition was triggered using 25 μM glibenclamide (Thermo Fisher) 30 min before infection. Finally, stimulations by leptospiral LPS were performed with 1 μg/mL of LPS of *L. interrogans* L495 extracted from the phenolic phase of the hot water/phenol extraction protocol, as we recently reviewed [22].

1.4. Immunofluorescence and high content (HC) automated microscopy

Cells were seeded and infected on cover glass (18 mm diameter, # 1.5 thickness, Electron Microscopy Science) and were fixed in 4 % v/v *para*-formaldehyde for 10 min, followed by three washes with PBS. Blocking was 1h in PBS +5 % w/v bovine serum albumin (BSA) and 2.5 μg/mL anti-CD16-CD32 (FcBlock, Thermo Fisher). Primary antibodies (Table 1) or isotypes were incubated overnight at 4 °C in PBS + 1 % w/v BSA, 0.05 % w/v saponin. Cells were then washed three times with PBS +0.05 % w/v saponin and labeled for 1h with secondary antibodies when necessary (Table 1) and 1 μg/mL DAPI in PBS + 1 % w/v BSA, 0.05 % w/v saponin. For NRF2 nuclear staining, permeabilization was performed in PBS +1 % w/v BSA, 0.5 % v/v Triton X-100 for 10 min prior to blocking. Image acquisition was performed on Leica SP5 confocal microscope (63x - 1.4 NA, oil immersion). Default settings were used and both UV and argon lasers were used at power between 10 and 30 %.

For high content (HC) automated microscopy, cells were seeded in dark, transparent bottom 96-well plates (Greiner, μClear) at 0.1×10^6 cells/mL. Cells were stained as described, except for RAW-mLC3-DiFluo that were fixed 10 min in cold ethanol/acetone (1:1). Imaging was performed on Opera Phenix (PerkinElmer) using confocal settings and 63X water-immersion objective (NA 1.15). Light source was kept at 20 to 50 % power and exposure time was set to obtain intensities 1000–5000. Automated acquisition allowed analysis of 500–1000 cells/well in technical triplicates for each experiment. Automated image analysis workflow and puncta quantification was performed using Columbus image data storage and analysis system (PerkinElmer), with the following steps: *(i)* import data; *(ii)* find nuclei with DAPI signal; *(iii)* find cytoplasm using target protein signal (p62/NRF2/F4/80); *(iv)* select cell population of interest if relevant (F4/80$^+$ peritoneal cells), *(v)* find spots if relevant (p62); *(vi)* formulate classical outputs: number of p62 puncta, NRF2 intensity in nucleus/cytoplasm; *(vii)* formulate calculated outputs: %p62 positive cells, NRF2 ratio, %NRF2 positive cells; *(viii)* save script and run batch analysis and *(ix)* export data.

1.5. SDS-PAGE and Western blot

For Western blot, cells were scrapped and centrifuged (400 g, 10 min). Pellets were resuspended in 50 μL of ice-cold RIPA lysis buffer supplemented with 1x complete Mini, EDTA-free proteases inhibition cocktail (Roche). Cells were lysed on ice for 15 min

Table 1
Antibodies list for immunofluorescence and Western blot analyses.

Application[a]	Target	Clonality[b]	Conjugated	Host	Dilution	Reference	Supplier
IF	**p62**	mAb	No	Rabbit	1:500	ab109012	Abcam
	Rabbit IgG	pAb	AlexaFluor 488	Goat	1:1.000	A-11034	ThermoFisher
IF	**Nrf2**	mAb	No	Rat	1:250	#14596	CST
	Rat IgG	pAb	AlexaFluor 647	Goat	1:1.000	A-21247	ThermoFisher
IF	**F4/80**	mAb	APC-Cyanine7	Rat	1:250	123117	BioLegend
WB	**LC3**	pAb	Purified	Rabbit	1:1.000	L7543	Sigma
	p62	mAb	Purified	Mouse	1:1.000	ab109012	Abcam
	OPTN	pAb	Purified	Rabbit	1:1.000	ab23666	Abcam
	NDP52	pAb	Purified	Rabbit	1:1.000	GTX115378	GeneTex
	Rabbit IgG	pAb	HRP	Goat	1:10.000	7074S	CST

[a] IF: immunofluorescence, WB: Western blot.
[b] mAb: monoclonal antibody, pAb: polyclonal antibody.

followed by centrifugation (12000 g, 40 min, 4 °C). Soluble proteins were recovered in the supernatant and dosed using the Bradford assay and the samples were denatured in Laemli buffer (99 °C, 10 min). SDS-PAGE was performed at 100 V on 4–15 % gradient acrylamide Stain-free gels in Tris-Glycine-SDS buffer (BioRad), with 5–10 μg of protein. Total proteins were visualized as internal control using stain free reagent in ChemiDoc (BioRad) with a 5 min exposition time and then transferred on 0.22 μm PVDF membrane (BioRad) using Mixed MW fast transfer of 1 miniGel (BioRad). Membrane was blocked 1h in TBS with 0.05 % v/v Tween 20 (TBS-T) + 5 % w/v BSA. The membrane was probed overnight at 4 °C with primary antibodies (Table 1) in TBS-T + 5 % w/v BSA. After three washes, membrane was incubated 1h with secondary anti-rabbit IgG HRP-linked (Table 1) in TBS-T + 5 % w/v BSA. After three washes, blots were revealed using the Clarity reagent (BioRad) with automatic exposure time.

1.6. Small interfering RNA transfection

For siRNA transfection, cells were seeded at confluence of 0.1×10^6 cells/mL the day before transfection. Transfection was performed using Lipofectamine siRNA Max reagent (ThermoFisher) OptiMEM media (Gibco) and according to the manufacturer's instructions. The final concentration of commercial predesigned siRNA targeting *p62* and *nrf2* (FlexiTube, Qiagen) was 80 nM and the corresponding scramble siRNA (all start negative, Qiagen) was used as control. The siRNA preparations in lipofectamine were incubated at room temperature for 25 min before delicate transfection of the cells in OptiMEM. After 8 h, the same volume of RPMIc was added for overnight incubation. Infection was performed the next day in RPMIc after complete media removal.

1.7. ELISA and Griess reaction

Fresh cell culture supernatants were used 24h post-infection for dosage of nitric oxide (NO) by the Griess reaction. Cytokine dosage was performed on frozen supernatants by ELISA using DuoSet kits (R&D Systems), according to the manufacturer's instructions. NO and cytokine concentrations were plotted both before and after normalization by cell viability.

1.8. Viability and LDH release assays

LDH release was measured using the CyQuant LDH Cytotoxicity Assay kit (fresh supernatant) (Invitrogen), according to the manufacturers' instructions. Viability was measured using MTT assay: cells were incubated for 2h in 1 mg/mL MTT solution (Sigma) in complete RPMI. MTT crystals were then dissolved in HCl 1 M, isopropanol (1:24) and absorbance was read at 595 nm. For each technical replicate, the viability value was used to normalize both NO and cytokines measurements using the following formula: $Normalized\ value = \frac{NO/cytokine\ value}{MTT\ value}$.

1.9. RT-qPCR

RNAs were extracted from frozen cells using RNeasy Mini Kit (Qiagen) according to the manufacturer's instructions. cDNAs were then obtained by retro-transcription (RT) using SuperScript II RT (Invitrogen). The equivalent of 20 ng of cDNA were used for RT-qPCR with specific primers and probes (Table 2). qPCR was performed using Taqman Universal MasterMix (Applied Biosystems) on a StepOne Plus Real Time PCR System (Applied Biosystems) with

Table 2
Primers and probe list for RT-qPCR analyses.

Target	Forward primer sequence	Reverse primer sequence	Probe sequence
p62	5'-ATGTGGAACATGGAGGGAAGAG-3'	5'-TTCTGTGCCTGTGCTGGAACT-3'	5'-CCGCCTGACACCCACTACCCCA-3'
lc3	5'-GCCCCACCCCTGAAAGG-3'	5'-TGCAGAGGAAATGACCACAGAT-3'	5'-TGGCTCCCCTTGTCCTGACTCGG-3'
iNOS	5'-CATGACTGCTAATGTCAGAG-3'	5'-TCCTAGTCCATCCGGATAAA-3'	5'-GAAATCTGAGTTTGGCCTGAGG-3'
tnf	5'-CATCTTCTCAAAATTCGAGTGACAA-3'	5'-TGGGAGTAGACAAGGTACAACCC-3'	5'-CACGTCGTAGCAAACCACCAAGTGGA-3'
il6	5'-CTCCAGCTTATCTGTTAGGA-3'	5'-CTTCAACCAAGAGGTAAAAGA-3'	5'-AAATTGGGGTAGGAAGGACTATTTTATG-3'
il10	5'-GGCGCTGTCATCGATTTCTC-3'	5'-GACACCTTGGTCTTGGAGCTTATTAA-3'	5'-AAAATAAGAGCAAGGCAGTGGAGCAGGTG-3'
hprt	5'-CTGGTGAAAAGGACCTCTCGA-3'	5'-TGCCCTTGACTATAATGAGTACTTCA-3	5'-TGTTGGATACAGGCCAGACTTTGTTGGAT-3'
cat	Pre-designed: Mm00437992_m1 (ThermoFisher)		
gsr	Pre-designed: Mm01197925_m1 (ThermoFisher)		
hprt	Pre-designed: Mm03024075_m1 (ThermoFisher)		

the standard protocol. Fold changes were calculated with the $2^{-\Delta\Delta CT}$ method, using hypoxanthine guanine phosphoribosyl transferase (HPRT) as internal control.

1.10. Statistical analyses

All statistical analyses were performed using Student's t-test with corresponding p values: * for $p < 0.05$; ** for $p < 0.01$ and *** for $p < 0.001$.

1.11. Ethics statement

All experiments performed on animals were conducted in accordance with the Animal Care guidelines and following the European Union Directive 2010/63 EU. Protocol was approved beforehand (#HA-0036) by the ethic committee of the Pasteur Institute, Paris, France (CETEA#89), in compliance with the French and European regulations on animal welfare and according to the Public Health Service recommendations.

2. Results

2.1. L. interrogans induces upregulation and specific accumulation of autophagy-adaptor p62 in puncta-like structures

To address modulation of autophagy-adaptors upon infection with leptospires, we infected bone marrow derived macrophages (BMDMs) with *L. interrogans* Manilae strain L495 and analyzed by Western blot the levels of the different adaptors p62, NDP52 and Optineurin. We observed an accumulation of p62 over time upon infection (Fig. 1A). We confirmed this phenotype using other pathogenic serotypes of *L. interrogans*: Copenhageni strain Fiocruz L1-130 and Icterohaemorrhagiae strain Verdun, and using the saprophytic *L. biflexa* Patoc strain Patoc I (Fig. 1B). Epifluorescence analyses of BMDMs infected 4h with *L. interrogans* further revealed that infection triggers accumulation of p62 in puncta-like structures (Fig. 1C). This phenotype seemed specific to p62 since we did not observe accumulation of the autophagy adaptors (NDP52 & optineurin) upon *Leptospira* infection (Sup. Fig. 2A).

Among other mechanisms, autophagy adaptors are constitutively degraded by autophagy upon autophagosome/lysosome fusion. We hypothesized that p62 accumulation could be triggered by blockage of autophagic flux by leptospires. However, when we monitored the autophagy hallmark protein LC3-II in BMDMs by Western blot, no LC3-II accumulation was observed upon *Leptospira* infection, in contrast to Bafilomycin (BafA1) treatment that blocks the autophagic flux, causing LC3-II to accumulate (Sup. Fig. 1A). Thus we conclude that infection with leptospires does not alter autophagic flux. Unexpectedly, we observed a mild reduction in LC3-II levels upon infection (Sup. Fig. 1B). Using murine macrophages RAW-mLC3-diFluo cells analyzed by automated microscopy, we were able to confirm that leptospires induce a mild decrease of the number of autophagosomes without altering the number of autolysosomes, again showing no alteration of the autophagic flux (Sup. Fig. 1C and D).

We then analyzed the transcriptional regulation of p62 in BMDMs by RT-qPCR and observed a significant upregulation of p62 mRNA 24 h post-infection with *L. interrogans* (Fig. 1D). This supported the idea that p62 accumulation is not mediated by autophagy blockage. The kinetics of the p62 puncta formation were further characterized in RAW264.7 cells, using automated high content (HC) confocal microscopy. We showed a time-dependent increase of both the number of p62 puncta *per* cell and the percentage of p62 positive cells (Fig. 1E & Sup. Fig. 2B). Single cell analysis confirmed an average of 5–10 puncta *per* cell and highlighted cell-to-cell heterogeneity, with some macrophages containing up to 60 puncta/cell (Fig. 1F). Of note, BafA1 that blocks autophagic flux also led to p62 accumulation as expected, but to a much lower extent than infection with leptospires (Fig. 1C, E & 1F). Conversely, the treatment of infected cells with rapamycin, a potent activator of the autophagy pathway, did not rescue the accumulation of p62 induced by leptospires (Sup. Fig. 2C). Altogether, these results confirm our previous results showing that *L. interrogans* do not induce autophagy in murine macrophages [14], and suggest that leptospires induce an autophagy-independent specific accumulation of p62.

2.2. p62 accumulation is triggered by the leptospiral LPS through TLR4 & TLR2

Many bacteria interfere actively with autophagy molecules *via* secreted effectors or RNA interference [16,23–28]. To investigate whether such active mechanisms are also used by leptospires, we analyzed BMDMs and RAW264.7 cells after stimulation with heat-killed (HK) leptospires. We observed p62 accumulation visible by Western blot (Fig. 2A) and quantified by automated microscopy (Fig. 2B & C). These findings excluded an active mechanism and suggested a role for the recognition of a leptospiral MAMP. Given its central role in the physiopathology of leptospirosis, we therefore stimulated cells for 24h with leptospiral LPS and observed that such stimulation recapitulates p62 accumulation (Fig. 2A, B & 2C). As p62 accumulation seemed to be mediated by recognition of the leptospiral LPS, we investigated the roles of TLR4 and TLR2. In murine cells, these two receptors are respectively activated by the leptospiral lipid A, and the leptospiral lipoproteins that co-purify with the LPS [5,12]. We infected WT and TLR2/4 dko BMDMs, that are no longer responsive to LPS, Pam2Cys and Pam3Cys (Sup. Fig. 3A), with *L. interrogans* and analyzed the p62 phenotype on each cell-type. We observed that p62 accumulation was greatly impaired in TLR2/TLR4 dko cells in response to both live and heat-killed bacteria, and purified LPS (Fig. 2D & E). Finally, we analyzed mRNA levels by RT-qPCR and observed that the increase in p62 mRNA levels observed in WT BMDMs was abolished in TLR2/4 dko BMDMs (Fig. 2F). Overall, these data showed that p62 accumulation is mediated by TLR2/4 recognition of the leptospiral LPS. To address if this phenotype is conserved *in vivo*, we injected C57BL/6 mice intraperitoneally with 1×10^8 heat-killed *L. interrogans*. Heat-killed leptospires are MAMPs and potent TLR2/TLR4 agonists, that present the advantage of not replicating nor disseminating upon injection. Interestingly, using automated microscopy we showed that p62 was also accumulated *in vivo* in peritoneal F4/80$^+$ macrophages (Fig. 2G).

Finally, we ask whether this mechanism of p62 accumulation could be conserved in human cells. Indeed, there is a TLR4 host species-specificity of the innate immune recognition of leptospires [29]. Leptospiral lipid A activates mouse-TLR4 but not human-TLR4 [12]. However, lipoproteins that co-purify with the LPS activate both mouse-TLR2 and human-TLR2 in a CD14-dependent manner [12]. We therefore infected human monocytic THP1-CD14 cells with *L. interrogans* serovar Manilae strain L495. We also observed a specific p62 accumulation and no NDP52 accumulation after infection with leptospires (Sup. Fig. 2D), suggesting conserved mechanism of p62 accumulation in human and murine macrophages, and a prominent role of TLR2 in human cells.

Leptospires have been shown to activate the NLRP3 inflammasome, in humans [30,31], and in mice in a TLR2/4-dependent manner [7]. Furthermore, NLRP inflammasomes have been shown to modulate autophagy [32–35]. Therefore, we asked whether activation of inflammasome could play a role in p62 accumulation and LC3-II diminution. We stimulated BMDMs with both live and

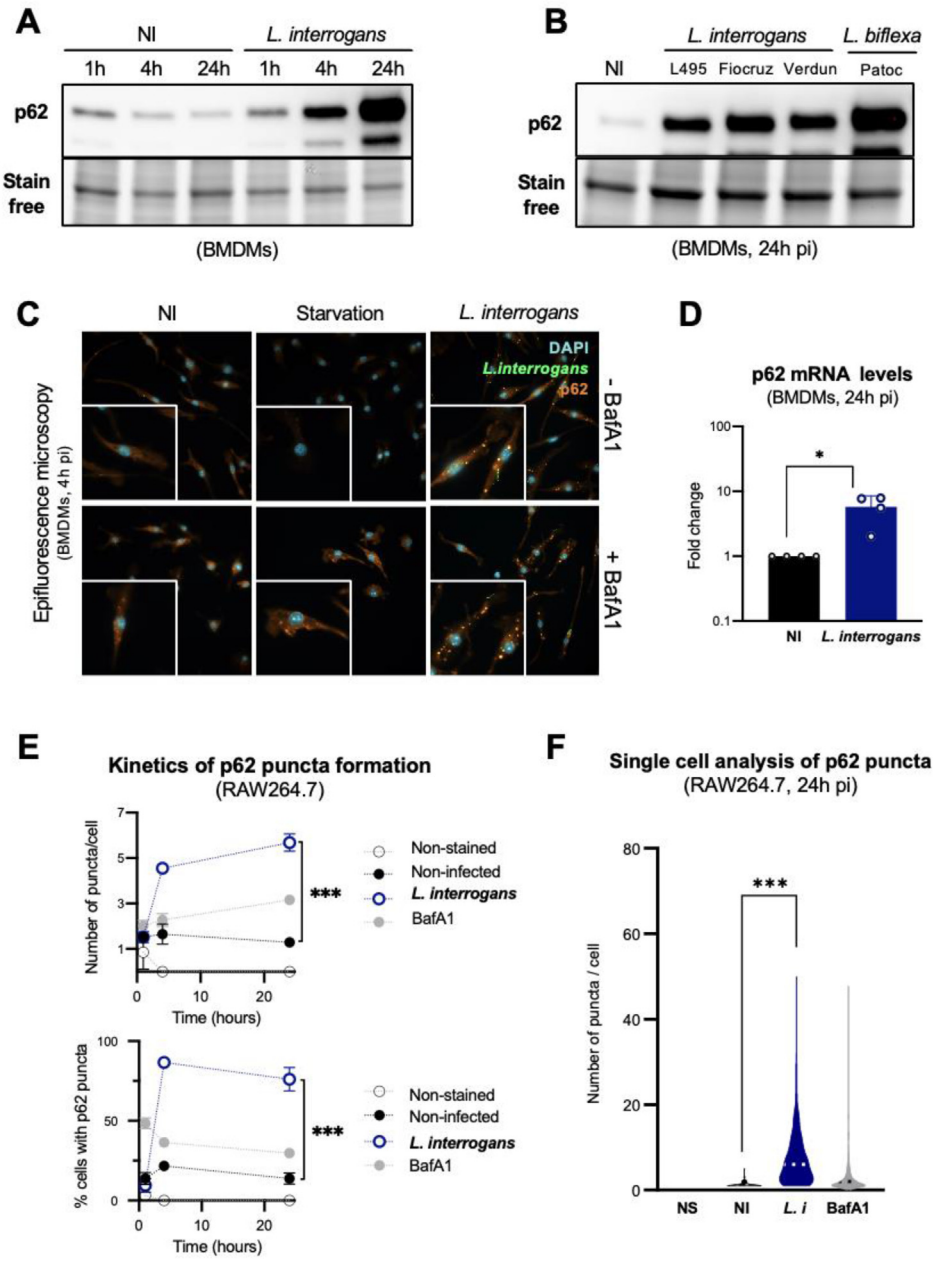

Fig. 1. *L. interrogans* induces upregulation and specific accumulation of autophagy-adaptor p62 in puncta-like structures. **A)** WB of p62 in BMDMs 1h, 4h and 24h post-infection with *L. interrogans* serovar Manilae strain L495 at MOI 100. Gel stain free is presented as loading control of total proteins. **B)** WB of p62 in BMDMs 24h post-infection with *L. interrogans* serovar Manilae strain L495, serovar Copenhageni strain Fiocruz L1-130, serovar Icterohaemorrhagiae strain Verdun, and *L. biflexa* serovar Patoc strain Patoc I, at MOI 100. **C)** Epifluorescence analyses of p62 in BMDMs 4h post-infection with fluorescently-labeled *L. interrogans* serovar Manilae strain L495 at MOI 10, or 4h upon starvation induction in EBSS medium, with or without 100 nM of bafilomycin A1 (BafA1). **D)** RT-qPCR analyses of p62 mRNA levels in BMDMs 24h post-infection with *L. interrogans* serovar Manilae strain L495 at MOI 100. Bars correspond to mean ± SD of technical replicates ($n = 4$). **E)** Automated confocal microscopy analyses of the number of p62 puncta *per* cell and the percentage of p62 positive cells in RAW264.7 cells 1h, 4h and 24h post-infection with *L. interrogans* serovar Manilae strain L495 at MOI 100, or stimulation with 100 nM of BafA1. Dots correspond to mean ± SD of technical replicates ($n = 3$). **F)** Single cell microscopy analysis of the number of p62 puncta *per* cell 24h post-infection of RAW264.7 cells with *L. interrogans* serovar Manilae strain L495 at MOI 100, or stimulation with 100 nM of BafA1. Dashed lines correspond to median. **A-F)** Data presented are representative of at least 3 independent experiments. Statistical analyses were performed using Student's *t*-test with corresponding *p* values:* for $p < 0.05$ and *** for $p < 0.001$.

heat-killed leptospires in the presence or absence of NLRP3 inhibitor glibenclamide. Efficiency of the treatment was controlled by 24h post-infection by measuring IL1β, a cytokine dependent of inflammasome-activation (Sup. Fig. 3B). p62 and LC3-II levels were analyzed by Western blot. We observed similar levels of p62 accumulation upon infection with either live or heat-killed leptospires in both control and glibenclamide treated cells (Sup. Fig. 3C). Consistently, the diminution of LC3-II upon infection was visible in both control and glibenclamide treated cells (Sup. Fig. 3C). Additionally, we analyzed the levels of p62 upon infection in RAW264.7 cells (that lack a functional inflammasome, and do not produce IL1β) and in RAW-ASC cells (stably transfected with inflammasome adaptor ASC, allowing IL1β production) (Sup. Fig. 3D). As expected, we observed that p62 accumulates similarly in both cell types upon infection with leptospires (Sup. Fig. 3E). Overall, this suggests that the modulation of autophagy players by leptospires, although TLR2/4-dependent, is not mediated by activation of the NLRP3 inflammasome.

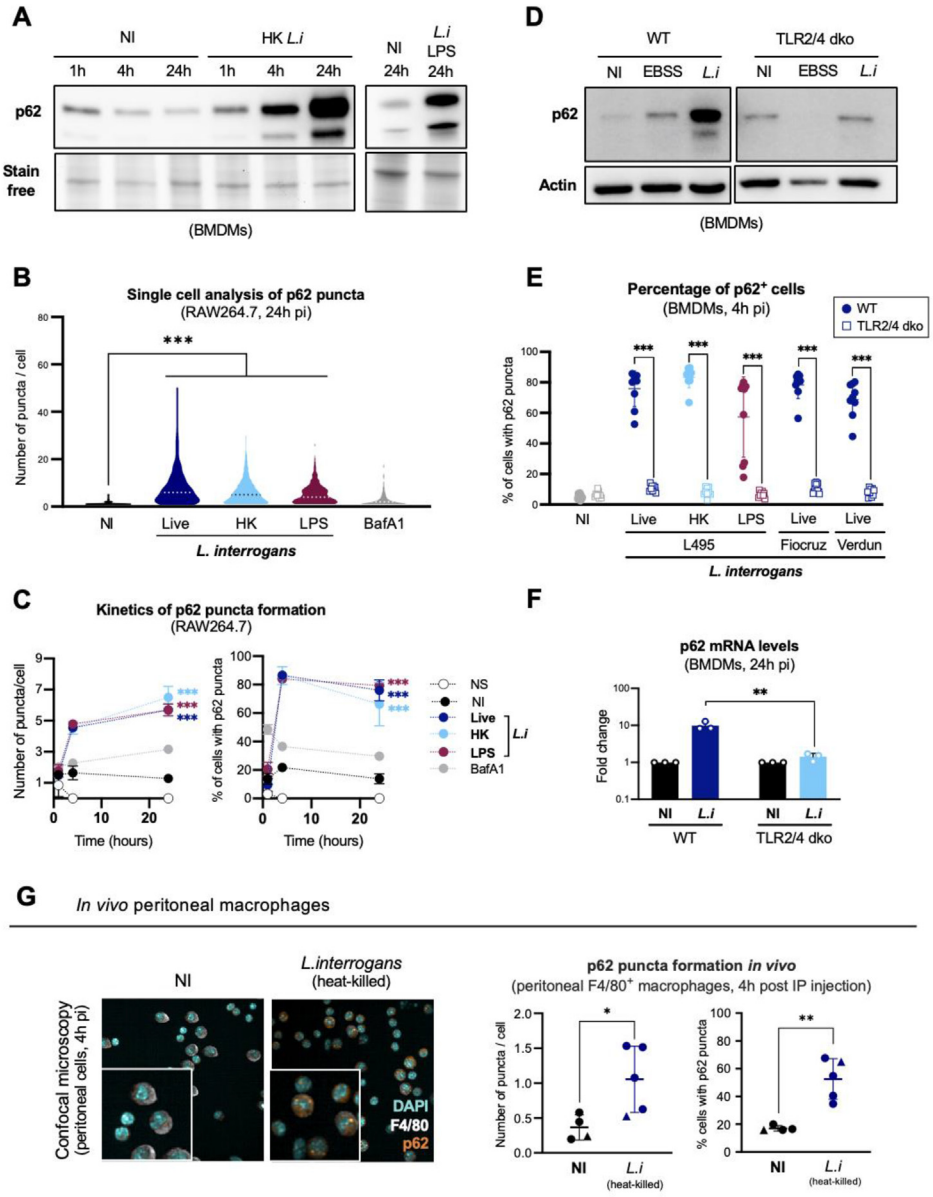

Fig. 2. p62 accumulation is triggered by the leptospiral LPS through TLR4 & TLR2 **A)** WB of p62 in BMDMs 1h, 4h and 24h post-stimulation with heat-killed (56 °C, 30 min) *L. interrogans* serovar Manilae strain L495 at MOI 100 or 24 h post-stimulation with 1 μg/mL of the corresponding purified leptospiral LPS. Gel stain free is presented as a loading control of total proteins. **B)** Single cell microscopy analysis of the number of p62 puncta *per* cell 24h post-infection of RAW264.7 cells with either live or heat-killed (56 °C, 30 min) *L. interrogans* serovar Manilae strain L495 at MOI 100, stimulation with 1 μg/mL of the corresponding purified leptospiral LPS, or stimulation with 100 nM of bafilomycin A1 (BafA1). Dashed lines correspond to median. **C)** Automated confocal microscopy analyses of the number of p62 puncta *per* cell and the percentage of p62 positive cells 1h, 4h and 24h post-stimulation of RAW264.7 cells with MOI 100 of either live or heat-killed (56 °C, 30 min) *L. interrogans* serovar Manilae strain L495, stimulation with 1 μg/mL of the corresponding purified leptospiral LPS, or stimulation with 100 nM of BafA1. Dots correspond to mean ± SD of technical replicates ($n = 3$). **D)** WB of p62 in WT and TLR2/4 dko BMDMs 24h post-infection with *L. interrogans* serovar Manilae strain L495 at MOI 100, or upon starvation induction in EBSS medium. WB of actin is presented as loading control. **E)** Automated confocal microscopy analyses of the percentage of p62 positive cells 4h post-stimulation of WT and TLR2/4 dko BMDMs with MOI 100 of *L. interrogans* serovar Manilae strain L495, serovar Copenhageni strain Fiocruz L1-130 or serovar Icterohaemorrhagiae strain Verdun or stimulation with heat-killed (56 °C, 30 min) bacteria or 1 μg/mL of the corresponding purified leptospiral LPS. Dots correspond to technical replicates pooled from three independent BMDMs preparations (n=3/mouse). **F)** RT-qPCR analyses of p62 mRNA levels in WT and TLR2/4 dko BMDMs 24h post-infection with *L. interrogans* serovar Manilae strain L495 at MOI 100. Bars correspond to mean of independent experiments ($n = 3$). **G)** Automated confocal microscopy images and analyses of the number of p62 puncta *per* cell and the percentage of p62 positive cells in adherent F4/80$^+$ peritoneal cells 4h post intra-peritoneal injection of 1×10^8 heat-killed (56 °C, 30 min) *L. interrogans* serovar Manilae strain L495 in C57BL/6J mice. Dots correspond to individual mice from 3 independent experiments (round = females/triangle = males). **A-G)** Data show or are representative of at least 3 independent experiments. Statistical analyses were performed using Student's *t*-test with corresponding *p* values: * for $p < 0.05$; ** for $p < 0.01$ and *** for $p < 0.001$.

2.3. Leptospiral LPS triggers nuclear translocation of the transcription factor NRF2

Stress pathways are induced when autophagy adaptors accumulate in the cell (i.e. in the absence of functional autophagy or because of specific upregulation). p62 accumulation induces translocation of stress-responsive nuclear factor erythroid 2-related factor 2 (NRF2) [20,36,37]. Subsequently, NRF2 triggers antioxidant and antiapoptotic programs [20,36], and promotes p62 upregulation, creating a loop that counteracts stress in autophagy-deficient conditions [36]. We therefore infected BMDMs with *L. interrogans* serovar Manilae strain L495 to analyze NRF2

localization by immunofluorescence 4h post-infection. Whilst NRF2 staining was barely visible in the non-infected conditions, it clearly appeared in cell nuclei upon infection (Fig. 3A), with a maximum of intensity that peaked around 4h post-infection (Fig. 3B). We performed single cell analysis of NRF2 fluorescence intensity in the nucleus of RAW264.7 cells infected for 4h with three different serovars of *L. interrogans*, and observed similar NRF2 increase for all the strains (Fig. 3C, *left panel*). We then calculated the ratio of nuclear to cytoplasm NRF2 and observed an increase in the ratio from 1.3 at basal state to 1.5 in infected cells (Fig. 3C, *right panel*). This allowed us to define a threshold at the intermediate value of 1.4 for NRF2 activated cells. The percentage of cells with NRF2 ratio >1.4 was plotted and we observed that up to 60 % of cells were positive 4h post-infection (Fig. 3C, *right panel*). To understand the contribution of leptospiral LPS in triggering NRF2, we performed similar analyses on cells stimulated for 4h with either live, heat-killed leptospires or their purified LPS and we observed that all conditions triggered similar NRF2 translocation (Fig. 3D). To confirm the contribution of the leptospiral LPS in NRF2 translocation, we analyzed WT and TLR2/4 dko BMDMs infected with *L. interrogans* (Fig. 3E) or stimulated with heat-killed leptospires or their purified LPS (Fig. 3F). As expected, we observed that the leptospiral-specific NRF2 translocation is reduced almost to baseline in TLR2/4 dko BMDMs. Altogether these data confirm that p62 accumulation and NRF2 translocation are dependent on leptospiral LPS signaling through TLR2/4.

Given the role played by the leptospiral LPS in the triggering of p62 accumulation and NRF2 translocation, we questioned whether

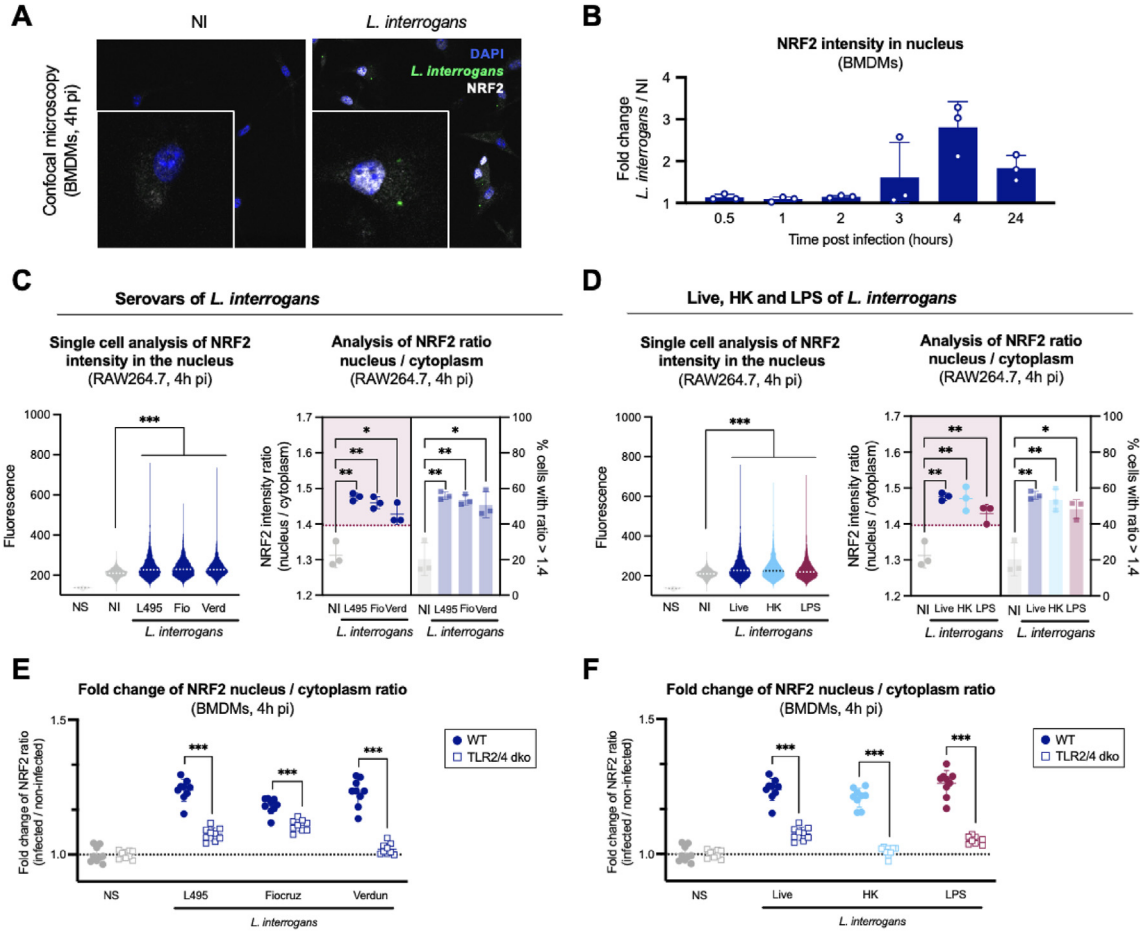

Fig. 3. Leptospires and their LPS trigger translocation of transcription factor NRF2 **A)** Confocal microscopy analyses of NRF2 in BMDMs 4h post-infection with *L. interrogans* serovar Manilae strain L495 at MOI 100. **B)** Automated confocal microscopy analyses of NRF2 intensity 0.5h, 1h, 2h, 4h and 24h post-infection of BMDMs with *L. interrogans* serovar Manilae strain L495 at MOI 100. Fluorescence values of infected cells were normalized by non-infected cells. Bars correspond to mean ± SD of technical replicates ($n = 3$). **C) Left panel.** Single cell microscopy analysis of NRF2 intensity in the nucleus 4h post-infection of RAW264.7 cells with *L. interrogans* serovar Manilae strain L495, serovar Copenhageni strain Fiocruz L1-130 or serovar Icterohaemorrhagiae strain Verdun at MOI 100. Fluorescence is expressed in arbitrary units (AU). Dashed lines correspond to median. **Right panel.** Automated confocal microscopy analysis of NRF2 intensity ratio [nucleus/cytoplasm] (*left axis*) and of the number of cells with NRF2 ratio >1.4 (*right axis*) 4h post-infection of RAW264.7 cells with *L. interrogans* serovar Manilae strain L495, serovar Copenhageni strain Fiocruz L1-130 or serovar Icterohaemorrhagiae strain Verdun at MOI 100. Lines correspond to mean ± SD of technical replicates ($n = 3$). **D) Left panel.** Single cell microscopy analysis of NRF2 intensity in the nucleus 4h post-infection of RAW264.7 cells with MOI 100 of either live or heat-killed (56 °C, 30 min) *L. interrogans* serovar Manilae strain L495 or stimulation with 1 μg/mL of the corresponding purified leptospiral LPS. Fluorescence is expressed in arbitrary units (AU). Dashed lines correspond to median. **Right panel.** Automated confocal microscopy analysis of NRF2 intensity ratio [nucleus/cytoplasm] (*left axis*) and of the number of cells with NRF2 ratio >1.4 (*right axis*) 4h post-infection of RAW264.7 cells with MOI 100 of either live or heat-killed (56 °C, 30 min) *L. interrogans* serovar Manilae strain L495 or stimulation with 1 μg/mL of the corresponding purified leptospiral LPS. Lines correspond to mean ± SD of technical replicates ($n = 3$). **E)** Automated confocal microscopy analysis of NRF2 [nucleus/cytoplasm] ratio fold change 4h post-infection of WT and TLR2/4 dko BMDMs with *L. interrogans* serovar Manilae strain L495, serovar Copenhageni strain Fiocruz L1-130 or serovar Icterohaemorrhagiae strain Verdun at MOI 100. Lines correspond to mean ± SD of technical replicates ($n = 3$). **F)** Automated confocal microscopy analysis of NRF2 [nucleus/cytoplasm] ratio fold change 4h post-infection of WT and TLR2/4 dko BMDMs with MOI 100 of either live or heat-killed (56 °C, 30 min) *L. interrogans* serovar Manilae strain L495 or stimulation with 1 μg/mL of the corresponding purified leptospiral LPS. Dots correspond to technical replicates pooled from three independent BMDMs preparations (n=3/mouse). **A-F)** Data show or are representative of at least 3 independent experiments. Statistical analyses were performed using Student's *t*-test with corresponding *p* values: * for $p < 0.05$; ** for $p < 0.01$ and *** for $p < 0.001$.

a pure TLR4 agonist would induce the same phenotypes. To answer this, we stimulated both WT and TLR2/4 dko BMDMs with ultrapure LPS from *E. coli* and we observed, as expected, a loss of accumulation of p62 and translocation of NRF2 in TLR2/4 dko BMDMs (Sup. Fig. 4A).

2.4. Leptospiral infection induces a p62/NFR2 activating feedback loop

Consequent to p62 accumulation and NRF2 translocation upon infection with *L. interrogans*, we investigated the potential regulation mechanisms between these two phenotypes. Using small-interfering RNA (siRNA) transfection in BMDMs to knock-down specifically p62 or NRF2, we analyzed NRF2 and p62 4h post-infection with leptospires by automated microscopy. We observed that the NRF2 ratio [nucleus/cytoplasm] was lower upon infection in the p62 siRNA condition (Fig. 4A, *left panel*). Conversely, p62 puncta formation was reduced upon infection in NRF2 siRNA transfected BMDMs (Fig. 4B, *left panel*). Both p62 and NRF2 knock-down were confirmed and quantified by automated microscopy (Fig. 4A & B, *right panels*). Overall, these results showed that p62 contributed to NRF2 translocation, and that, in turn, NRF2 regulated p62 puncta formation, suggesting that p62 and NRF2 are in a feedback loop upon infection by *L. interrogans*.

To further characterize the connection of NRF2 in p62 activation, we analyzed BMDMs transfected with NRF2 siRNA and infected with *L. interrogans* by Western blot and RT-qPCR 24h post-infection, allowing us to measure both the protein and mRNA levels of p62. Interestingly, we observed that NRF2 silencing prevented p62 protein accumulation (Fig. 4C) but also reduced mRNA upregulation (Fig. 4D), suggesting that NRF2 is a transcriptional regulator of p62 activation.

2.5. NRF2 translocation prevents inflammation upon infection

NRF2 is a stress response transcription factor that promotes antioxidant and antiapoptotic programs upon activation [20,36]. Therefore, we monitored the transcription of targets genes involved in fighting oxidative stress in macrophages in response to infection. We infected BMDMs with *L. interrogans* and analyzed the levels of

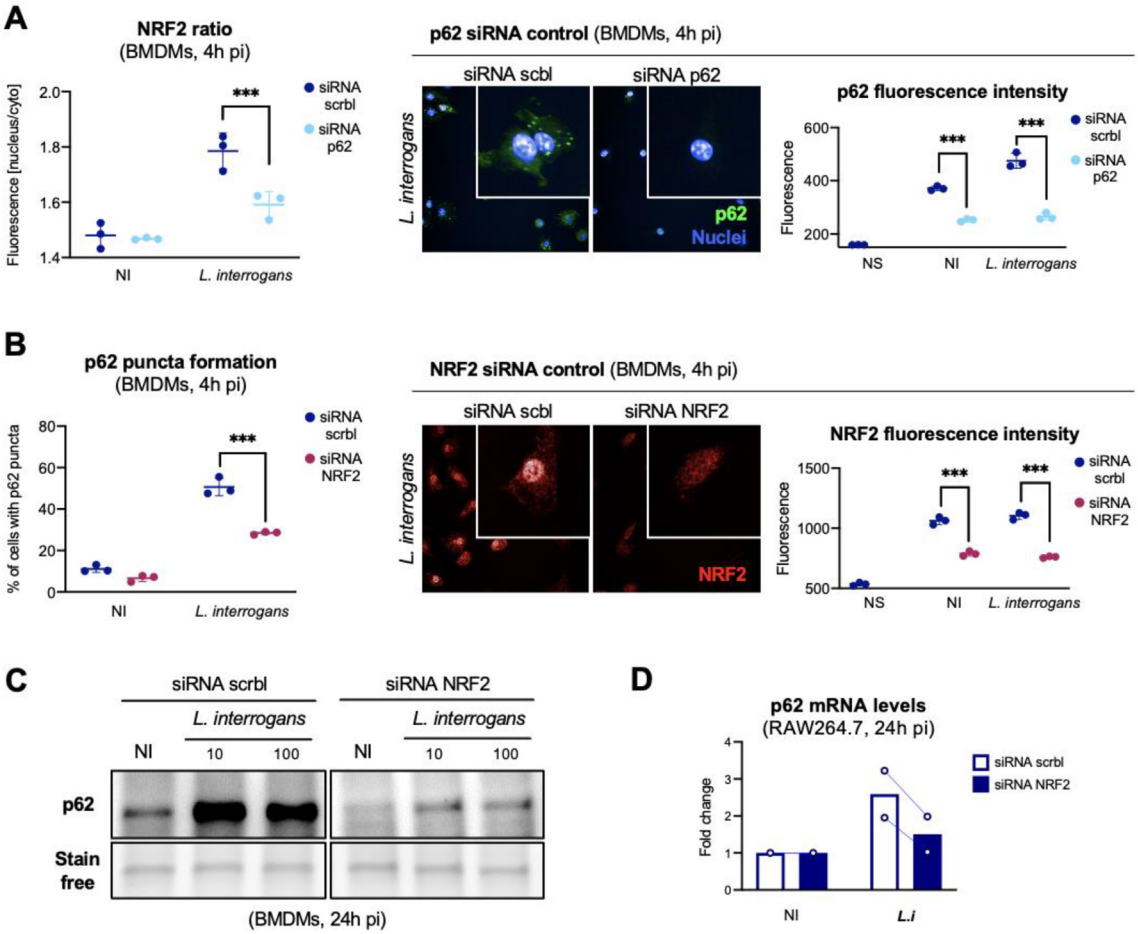

Fig. 4. p62 and NRF2 are in a feedback loop upon infection with leptospires **A) Left panel.** Automated confocal microscopy analysis of NRF2 intensity ratio [nucleus/cytoplasm] in BMDMs transfected with scramble (scrbl) or p62 siRNA and infected for 4h with *L. interrogans* serovar Manilae strain L495 at MOI 100. Lines correspond to mean ± SD of technical replicates ($n = 3$). **Right panel.** Corresponding controls are microscopy analyses and quantification of p62 intensity in the same transfection and infection conditions. Lines correspond to mean ± SD of technical replicates ($n = 3$). **B) Left panel.** Automated confocal microscopy analysis of p62 puncta formation in BMDMs transfected with scrbl or NRF2 siRNA and infected for 4h with *L. interrogans* serovar Manilae strain L495 at MOI 100. Lines correspond to mean ± SD of technical replicates ($n = 3$). **Right panel.** Corresponding controls are microscopy analyses and quantification of NRF2 intensity in the same transfection and infection conditions. Lines correspond to mean ± SD of technical replicates ($n = 3$). **C)** WB of p62 in BMDMs transfected with scrbl or NRF2 siRNA and infected for 24h with *L. interrogans* serovar Manilae strain L495 at MOI 10 or 100. **D)** RT-qPCR analyses of p62 mRNA levels in RAW264.7 cells transfected with scrbl or NRF2 siRNA and infected for 24h with *L. interrogans* serovar Manilae strain L495 at MOI 100. Bars correspond to mean of independent experiments ($n = 2$). **A-B)** Data presented are representative of at least 3 independent experiments. **C-D)** Data presented are representative of 2 independent experiments. Statistical analyses were performed using Student's *t*-test with corresponding *p* values: *** for $p < 0.001$.

glutathione S-reductase, catalase and heme oxygenase 1 mRNA by RT-qPCR at 4 h and 24 h post-infection. Interestingly, we observed no upregulation of these transcripts (Sup. Fig. 5A, B & 5C), suggesting that no antioxidant program is activated upon infection with *L. interrogans*.

NRF2 has also been shown to have repressor functions and to dampen inflammation by inhibiting the transcription of cytokines [38,39], hence conferring resistance to inflammatory disease such as sepsis [38]. We therefore investigated the role of NRF2 translocation in inflammation upon infection by leptospires. We

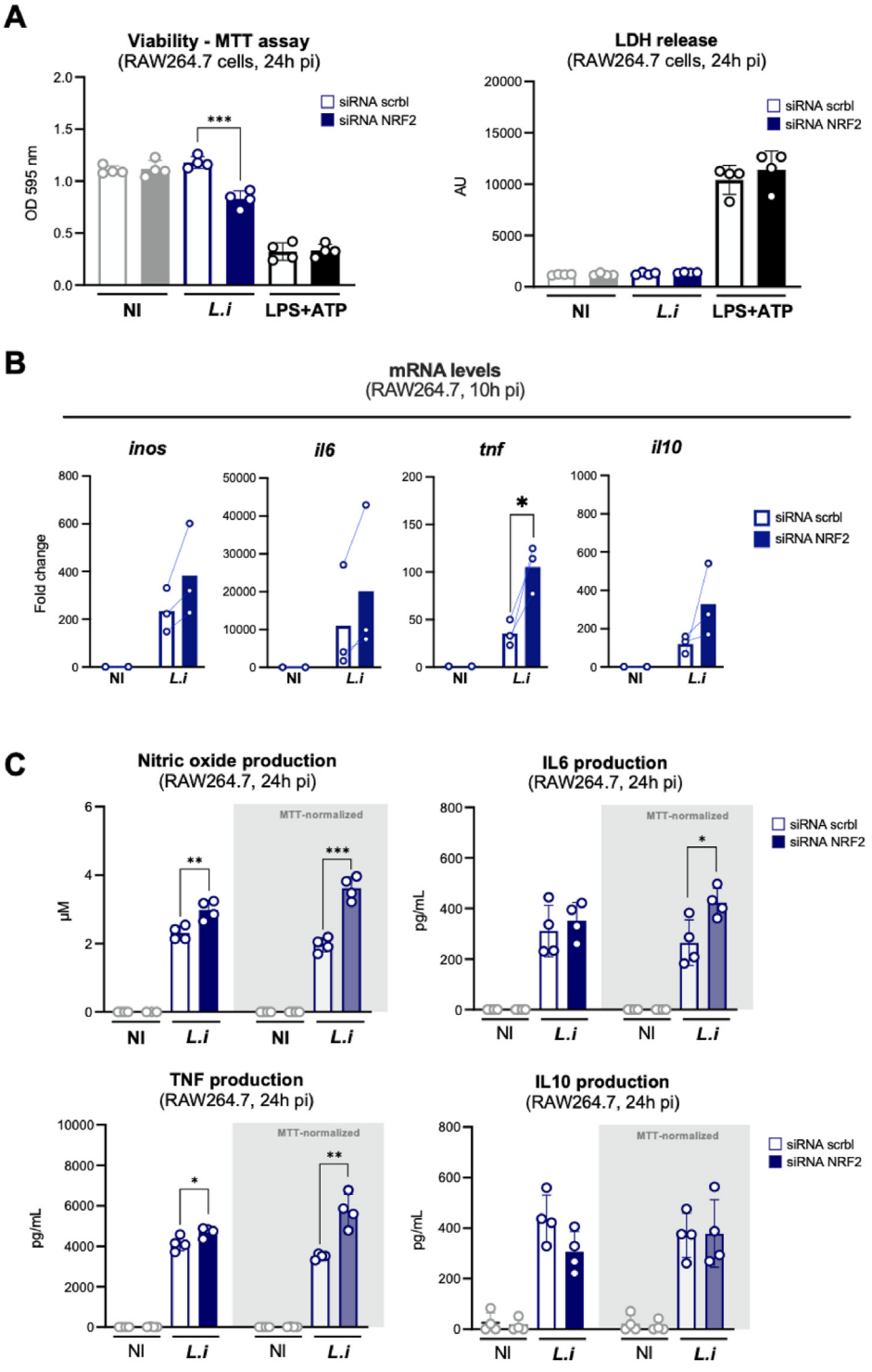

Fig. 5. NRF2 translocation prevents inflammation upon infection **A)** Cell viability (measured by MTT assay) and LDH release (measured by CyQuant assay) in RAW264.7 cells transfected with scramble (scrbl) or NRF2 siRNA and infected for 24h with *L. interrogans* serovar Manilae strain L495 at MOI 100 or stimulated with positive control for lytic cell death: LPS of *E. coli* 1 µg/mL + ATP 5 mM. Bars correspond to mean ± SD of technical replicates ($n = 4$). **B)** RT-qPCR analyses of iNOS, IL6, TNF and IL10 mRNA levels in RAW264.7 cells transfected with scrbl or NRF2 siRNA and infected for 10h with *L. interrogans* serovar Manilae strain L495 at MOI 100. Bars correspond to mean of independent experiments ($n = 3$). **C)** NO dosage by Griess reaction and, IL6, TNF and IL10 dosages by ELISA in RAW264.7 cells transfected with scrbl or NRF2 siRNA and infected for 24h with *L. interrogans* serovar Manilae strain L495 at MOI 100. Bars correspond to mean ± SD of technical replicates ($n = 4$). **A-C)** Data presented are representative of at least 3 independent experiments. Statistical analyses were performed using Student's *t*-test with corresponding *p* values: * for $p < 0.05$; ** for $p < 0.01$ and *** for $p < 0.001$.

transfected RAW264.7 cells with siRNA targeted against NRF2 and then infected them with *L. interrogans*. As expected, considering that NRF2 is known to prevent cell death, we observed a decrease in macrophage viability only upon infection of NRF2-silenced cells (Fig. 5A, *left panel*). Interestingly, this enhanced loss of viability was not associated with lactate dehydrogenase (LDH) release from the cytosol, illustrating that no membrane damage or cell lysis occurred (Fig. 5A, *right panel*). We then analyzed the mRNA levels of several cytokines and enzymes, namely iNOS (nitric oxide inducible synthase), IL6, TNF and IL10. Upon infection, *tnf* mRNA levels were significantly higher in NRF2-silenced cells than in control cells (Fig. 5B). The same trend was visible for *inos*, *il6* and *il10* transcripts (Fig. 5B), suggesting that NRF2 does play a role in repressing the expression of inflammatory targets. Finally, to address whether this transcriptional regulation was strong enough to alter cytokines levels, we analyzed nitric oxide (NO), IL6, TNF and IL10 production in cell supernatant. Consistent with the mRNA analyses, we observed higher NO and TNF upon infection of NRF2-silenced RAW264.7 (Fig. 5C). These findings were even more striking after normalizing cytokine production against cell viability, as measured using MTT (Fig. 5C, *grey areas*). Increased levels of IL6 were observed after normalizing for cell viability, whereas IL10 was not increased under any condition (Fig. 5C, *grey areas*). Interestingly, we also observed NRF2 knockdown-induced increased NO production in response to stimulation with ultra-pure LPS of *E. coli* (Sup. Fig. 4B). Overall, our results show that NRF2 plays a repressor role to dampen production of inflammatory mediators such as NO, TNF and IL6 in mouse macrophages upon infection with *L. interrogans*.

3. Discussion

Our results provide evidence for an accumulation of the autophagy adaptor p62 in puncta-like structures in response to infection with both pathogenic *L. interrogans* and saprophytic *L. biflexa*. Classically, the autophagy adaptor p62 accumulates on the surface of intracellular bacteria, such as *Salmonella* [16], *Listeria* or *Shigella* [40]. This targets bacterial cargo to autophagosomes and it is associated with active modulation of the autophagic flux through effectors [15,16,23,27,28]. However, in the case of *Leptospira*, we have previously reported that leptospires actively enter but do not remain inside macrophages and are not targeted by xenophagy [14]. Moreover, the accumulation of p62 is also visible in response to stimulation with extracellular heat-killed leptospires or with purified LPS through TLR2/TLR4, hence excluding that only intracellular leptospires actively promote the formation of p62 puncta. This hypothesis is consistent with the fact that leptospires do not possess traditional secretion systems [41] often used by other bacterial pathogens to modulate autophagy. Furthermore, our results showed that leptospires did not alter autophagic flux in macrophages. These findings are aligned with previous studies from our laboratory showing that leptospires escape different innate immune autophagy-activating pathways [15,42], such as NOD-like receptors [8] and TLR4-TRIF [13]. Overall, we conclude that the leptospires behave differently from other pathogenic bacteria that actively modulate autophagy, and for which p62 accumulates on the surface of intracellular bacteria.

We further demonstrated that p62 accumulation was induced by leptospiral LPS signaling through TLR2/TLR4. The unique leptospiral LPS, its best characterized and major virulence factor [10], plays an important role in leptospiral host–pathogen interactions. We previously showed that leptospiral LPS avoids human TLR4 and mouse TLR4-TRIF activation [13]. Recently, leptospiral LPS has also been shown to prevent cell death by pyroptosis [43]. In the present study, we found that the leptospiral LPS is responsible for the p62-puncta phenotype. Interestingly, the LPS of *L. biflexa* has been shown to be a more potent TLR4 agonist than the LPS of pathogenic *L. interrogans* [13], consistent with our results showing greater p62 accumulation observed after infection with the saprophytic strain. Overall, these findings are consistent with other studies reporting that p62 accumulates *via* TLR signaling [44], directly through NFκB-mediated transcriptional regulation. We believe this could be the case upon infection with leptospires because: *(i)* our results show an upregulation of p62 mRNA upon infection and *(ii)* p62 levels upon infection are much higher than upon autophagy blockage with BafA1, suggesting that the accumulation of p62 is not mediated by a dysregulation of autophagy.

TLR-induced accumulation of p62 has been shown to trigger the translocation of the transcription factor NRF2 [44]. Under physiological conditions, NRF2 is classically targeted for degradation by the proteasome *via* interaction with its inhibitor Keap1 [37,45]. The accumulation and direct binding of p62 to Keap1, leads to its sequestration and subsequent release from NRF2, which then can translocate in the nucleus [20,36,37,45]. Our results confirmed that p62 induces translocation of NRF2 upon infection with leptospires, and illustrated that the feedback loop between p62 and NRF2, described in the literature [36], is activated upon *L. interrogans* infection. Interestingly, this loop has few negative regulators, and it is hypothesized that its main regulator would be autophagy, through degradation of p62 [36]. Therefore, we hypothesize that since infection with leptospires does not trigger autophagy, the feedback loop between p62 and NRF2 remains active, explaining why p62 puncta did not disappear even at 24h post-infection. Overall, out data indicate that leptospires are potent activators of the p62/NRF2 axis in macrophages.

Interestingly, NRF2 has also been shown to have transcription inhibition properties. In BMDMs, NRF2 was described as an inhibitor of transcription for pro-inflammatory targets such as IL6, IL1β and IL12 [39,46]. Our results showed that this is also the case upon infection with *L. interrogans*. NRF2 inhibits polymerase III recruitment and hence prevents transcription of cytokines in response to stimulation [39]. Consequently, NRF2 was shown to downregulate neutrophil activation and migration [47]. Interestingly, although neutrophils are abundant in the blood of mice and humans infected with leptospires, they are barely observed in the kidneys, the niche occupied by leptospires during chronic infection [48,49]. Whether *Leptospira* modulate NRF2 translocation in neutrophils *via* their LPS to favor survival in the kidneys remains to be studied. In addition, we showed that the accumulation of p62 observed in murine macrophages was conserved in human cells. Interestingly, human cells do not sense leptospiral lipid A through TLR4 [12], leading us to hypothesize that TLR2 alone could be responsible for sensing leptospires and inducing p62 accumulation in THP1 cells. Although we could not address NRF2 translocation in human cells due to lack of specific tools, we speculate that inflammation dampening might be conserved in human macrophages.

Other microbes such as Epstein–Barr virus (EBV) or parasite *Leshmania major* have been shown to activate the p62/NRF2 axis [50,51], hence indicating an important role of NRF2 in response to pathogens. However, to date, the role of NRF2 translocation in response to pathogens remains unclear. Among others, NRF2 is involved in the induction of antioxidant program upon infection [36]. We were therefore surprised to observe no modulation in the mRNA levels of antioxidant targets upon infection. Of note, pathogenic leptospires are equipped to fight against oxidative stress with inducible catalase, a virulent factor, peroxidase, and peroxiredoxin [52]. Interestingly, active repression of these NRF2-dependent antioxidant targets was previously shown upon infection with live *L. major* parasite [51,53]. Whether leptospires could also actively prevent upregulation of NRF2 antioxidant targets remains to be addressed.

In summary, we have demonstrated that leptospires passively subvert the p62-NRF2 axis through LPS activation of TLR signaling and this leads to a reduction of inflammatory mediators. This original mechanism might play a key role in the discretion of leptospires in hosts, evasion of immune cell recruitment, and could potentially contribute to the establishment of chronic infections.

Statement of ethics

All protocols were undertaken in compliance with EU Directive 2010/63 EU and the French regulation on the protection of laboratory animals issued on February 1st, 2013. They are part of project number # 2014-0049 and HA0036, which were approved by the Institut Pasteur ethics committee for animal experimentation (Comité d'Ethique en Expérimentation Animale CETEA registered under #89) and was authorized under #8562 by the French Ministry of Research, the French Competent Authority.

Funding sources

This work was funded by Institut Pasteur grant PTR2017-66 to CW and by Agence Nationale de la Recherche (ANR) grant ANR-10-LABX-62-IBEID to IGB. DB was funded by Université Paris Cité (formerly Université Paris Diderot) through Doctoral school FIRE (ED FIRE474). IS was part of the Pasteur-Paris University (PPU) International PhD program. This program received funding from the Institut Carnot Pasteur Microbes & Santé, and the European Union's Horizon 2020 research and innovation program under the Marie Sklodowska-Curie grant agreement no. 665807. IS additionally benefited from a scholarship "Fin de thèse de science" number FDT201805005258 granted by "Fondation pour la recherche médicale (FRM)". SP was supported by Université Paris Cité (formerly Université Paris Descartes) through doctoral school BioSPC (ED BIOSPC). The PE research was funded by the DARRI-Institut Carnot-Microbe et santé (grant number INNOV-SP10-19) and the ANR grant ANR-21-CE15-0038-01. France-BioImaging infrastructure network is supported by the French National Research Agency (ANR-10—INSB—04, Investments for the future). The use of the Opera Phenix system in the PBI core facility was made possible by the kind financial support of the Institut Pasteur (Paris) and the Région Ile-de-France (program DIM1Health).

Authors contributions

Conception, administration, and supervision of the project: CW.
Investigation: DB, IS, SP and CW.
Methodology: IS, DB and PE.
Data analysis: DB, IS, PE and CW.
Visualization: DB.
Validation: IS, DB, SP and CW.
Resources: FVP.
Funding acquisition: CW and IGB.
Revisions: DB, SP and CW.
DB and IS wrote the original draft, under CW's supervision.
All authors contributed to the review of the manuscript and approved it for submission.

Data availability statement

All data generated or analysed during this study are included in this article. Further enquiries can be directed to the corresponding author.

Declaration of competing interest

The authors have no conflicts of interest to declare.

Acknowledgments

We acknowledge Nathalie Aulner and Anne Danckaert (Institut Pasteur) as well as the Photonic BioImaging Unit of Technology and Service, a member of the France-BioImaging infrastructure, for support in conducting this study. We thank Richard Wheeler (Institut Pasteur) for critical reading of the manuscript and English editing.

Appendix A. Supplementary data

Supplementary data to this article can be found online at https://doi.org/10.1016/j.micinf.2023.105274.

References

[1] Costa F, Hagan JE, Calcagno J, Kane M, Torgerson P, Martinez-Silveira MS, et al. Global morbidity and mortality of leptospirosis: a systematic review. PLoS Neglected Trop Dis 2015;9(9):e0003898.
[2] Adler B. History of leptospirosis and *Leptospira*. Curr Top Microbiol Immunol 2015;387:1—9.
[3] Ko AI, Goarant C, Picardeau M. *Leptospira*: the dawn of the molecular genetics era for an emerging zoonotic pathogen. Nat Rev Microbiol 2009;7(10):736—47.
[4] Ratet G, Veyrier FJ, Fanton d'Andon M, Kammerscheit X, Nicola MA, Picardeau M, et al. Live imaging of bioluminescent *Leptospira interrogans* in mice reveals renal colonization as a stealth escape from the blood defenses and antibiotics. PLoS Neglected Trop Dis 2014;8(12):e3359.
[5] Werts C, Tapping RI, Mathison JC, Chuang TH, Kravchenko V, Saint Girons I, et al. Leptospiral lipopolysaccharide activates cells through a TLR2-dependent mechanism. Nat Immunol 2001;2(4):346—52.
[6] Hsu SH, Hung CC, Chang MY, Ko YC, Yang HY, Hsu HH, et al. Active components of *Leptospira* outer membrane protein LipL32 to toll-like receptor 2. Sci Rep 2017;7(1):8363.
[7] Lacroix-Lamande S, d'Andon MF, Michel E, Ratet G, Philpott DJ, Girardin SE, et al. Downregulation of the Na/K-ATPase pump by leptospiral glycolipoprotein activates the NLRP3 inflammasome. J Immunol 2012;188(6):2805—14.
[8] Ratet G, Santecchia I, Fanton d'Andon M, Vernel-Pauillac F, Wheeler R, Lenormand P, et al. LipL21 lipoprotein binding to peptidoglycan enables *Leptospira interrogans* to escape NOD1 and NOD2 recognition. PLoS Pathog 2017;13(12):e1006725.
[9] Holzapfel M, Bonhomme D, Cagliero J, Vernel-Pauillac F, Fanton d'Andon M, Bortolussi S, et al. Escape of TLR5 recognition by *Leptospira spp.*: a rationale for atypical endoflagella. Front Immunol 2020;11:2007.
[10] Murray GL, Srikram A, Henry R, Hartskeerl RA, Sermswan RW, Adler B. Mutations affecting *Leptospira interrogans* lipopolysaccharide attenuate virulence. Mol Microbiol 2010;78(3):701—9.
[11] Que-Gewirth NL, Ribeiro AA, Kalb SR, Cotter RJ, Bulach DM, Adler B, et al. A methylated phosphate group and four amide-linked acyl chains in *Leptospira interrogans* lipid A. The membrane anchor of an unusual lipopolysaccharide that activates TLR2. J Biol Chem 2004;279(24):25420—9.
[12] Nahori MA, Fournie-Amazouz E, Que-Gewirth NS, Balloy V, Chignard M, Raetz CR, et al. Differential TLR recognition of leptospiral lipid A and lipopolysaccharide in murine and human cells. J Immunol 2005;175(9):6022—31.
[13] Bonhomme D, Santecchia I, Vernel-Pauillac F, Caroff M, Germon P, Murray G, et al. Leptospiral LPS escapes mouse TLR4 internalization and TRIF-associated antimicrobial responses through O-antigen and associated lipoproteins. PLoS Pathog 2020;16(8):e1008639.
[14] Santecchia I, Bonhomme D, Papadopoulos S, Escoll P, Giraud-Gatineau A, Moya-Nilges M, et al. Alive pathogenic and saprophytic leptospires enter and exit human and mouse macrophages with No intracellular replication. Front Cell Infect Microbiol 2022;12:936931.
[15] Travassos LH, Carneiro LA, Girardin S, Philpott DJ. Nod proteins link bacterial sensing and autophagy. Autophagy 2010;6(3):409—11.
[16] Birmingham CL, Smith AC, Bakowski MA, Yoshimori T, Brumell JH. Autophagy controls *Salmonella* infection in response to damage to the *Salmonella*-containing vacuole. J Biol Chem 2006;281(16):11374—83.
[17] Gutierrez MG, Master SS, Singh SB, Taylor GA, Colombo MI, Deretic V. Autophagy is a defense mechanism inhibiting BCG and *Mycobacterium tuberculosis* survival in infected macrophages. Cell 2004;119(6):753—66.
[18] Miyashita H, Oikawa D, Terawaki S, Kabata D, Shintani A, Tokunaga F. Crosstalk between NDP52 and LUBAC in innate immune responses, cell death, and xenophagy. Front Immunol 2021;12:635475.

[19] Moscat J, Diaz-Meco MT, Wooten MW. Of the atypical PKCs, Par-4 and p62: recent understandings of the biology and pathology of a PB1-dominated complex. Cell Death Differ 2009;16(11):1426–37.
[20] Komatsu M, Kurokawa H, Waguri S, Taguchi K, Kobayashi A, Ichimura Y, et al. The selective autophagy substrate p62 activates the stress responsive transcription factor NRF2 through inactivation of Keap1. Nat Cell Biol 2010;12(3):213–23.
[21] Santecchia I, Vernel-Pauillac F, Rasid O, Quintin J, Gomes-Solecki M, Boneca IG, et al. Innate immune memory through TLR2 and NOD2 contributes to the control of *Leptospira interrogans* infection. PLoS Pathog 2019;15(5):e1007811.
[22] Bonhomme D, Werts C. Purification of LPS from *Leptospira*. Methods Mol Biol 2020;2134:53–65.
[23] Birmingham CL, Canadien V, Gouin E, Troy EB, Yoshimori T, Cossart P, et al. *Listeria monocytogenes* evades killing by autophagy during colonization of host cells. Autophagy 2007;3(5):442–51.
[24] Case ED, Chong A, Wehrly TD, Hansen B, Child R, Hwang S, et al. The *Francisella* O-antigen mediates survival in the macrophage cytosol via autophagy avoidance. Cell Microbiol 2014;16(6):862–77.
[25] Kreibich S, Emmenlauer M, Fredlund J, Ramo P, Munz C, Dehio C, et al. Autophagy proteins promote repair of endosomal membranes damaged by the *Salmonella* type three secretion system 1. Cell Host Microbe 2015;18(5):527–37.
[26] Chen Z, Wang T, Liu Z, Zhang G, Wang J, Feng S, et al. Inhibition of autophagy by MiR-30A induced by *Mycobacteria tuberculosis* as a possible mechanism of immune escape in human macrophages. Jpn J Infect Dis 2015;68(5):420–4.
[27] Choy A, Dancourt J, Mugo B, O'Connor TJ, Isberg RR, Melia TJ, et al. The *Legionella* effector RavZ inhibits host autophagy through irreversible Atg8 deconjugation. Science 2012;338(6110):1072–6.
[28] Ogawa M, Yoshimori T, Suzuki T, Sagara H, Mizushima N, Sasakawa C. Escape of intracellular *Shigella* from autophagy. Science 2005;307(5710):727–31.
[29] Bonhomme D, Werts C. Host and species-specificities of pattern recognition receptors upon infection with *Leptospira interrogans*. Front Cell Infect Microbiol 2022;12:932137.
[30] Li S, Wang M, Ojcius DM, Zhou B, Hu W, Liu Y, et al. Corrigendum to "*Leptospira interrogans* infection leads to IL-1beta and IL-18 secretion from a human macrophage cell line through reactive oxygen species and cathepsin B mediated-NLRP3 inflammasome activation" [Microbe Infect (2018) 254-260]. Microb Infect 2021;23(1):104756.
[31] Li S, Wang M, Ojcius DM, Zhou B, Hu W, Liu Y, et al. *Leptospira interrogans* infection leads to IL-1beta and IL-18 secretion from a human macrophage cell line through reactive oxygen species and cathepsin B mediated-NLRP3 inflammasome activation. Microb Infect 2018;20(4):254–60.
[32] Wlodarska M, Thaiss CA, Nowarski R, Henao-Mejia J, Zhang JP, Brown EM, et al. NLRP6 inflammasome orchestrates the colonic host-microbial interface by regulating goblet cell mucus secretion. Cell 2014;156(5):1045–59.
[33] Jounai N, Kobiyama K, Shiina M, Ogata K, Ishii KJ, Takeshita F. NLRP4 negatively regulates autophagic processes through an association with beclin1. J Immunol 2011;186(3):1646–55.
[34] Deng Q, Wang Y, Zhang Y, Li M, Li D, Huang X, et al. *Pseudomonas aeruginosa* triggers macrophage autophagy to escape intracellular killing by activation of the NLRP3 inflammasome. Infect Immun 2016;84(1):56–66.
[35] Lai M, Yao H, Shah SZA, Wu W, Wang D, Zhao Y, et al. The NLRP3-caspase 1 inflammasome negatively regulates autophagy via TLR4-TRIF in prion peptide-infected microglia. Front Aging Neurosci 2018;10:116.
[36] Jain A, Lamark T, Sjottem E, Larsen KB, Awuh JA, Overvatn A, et al. p62/SQSTM1 is a target gene for transcription factor NRF2 and creates a positive feedback loop by inducing antioxidant response element-driven gene transcription. J Biol Chem 2010;285(29):22576–91.
[37] Lau A, Wang XJ, Zhao F, Villeneuve NF, Wu T, Jiang T, et al. A noncanonical mechanism of Nrf2 activation by autophagy deficiency: direct interaction between Keap1 and p62. Mol Cell Biol 2010;30(13):3275–85.
[38] Kong X, Thimmulappa R, Craciun F, Harvey C, Singh A, Kombairaju P, et al. Enhancing Nrf2 pathway by disruption of Keap1 in myeloid leukocytes protects against sepsis. Am J Respir Crit Care Med 2011;184(8):928–38.
[39] Kobayashi EH, Suzuki T, Funayama R, Nagashima T, Hayashi M, Sekine H, et al. Nrf2 suppresses macrophage inflammatory response by blocking proinflammatory cytokine transcription. Nat Commun 2016;7:11624.
[40] Mostowy S, Sancho-Shimizu V, Hamon MA, Simeone R, Brosch R, Johansen T, et al. p62 and NDP52 proteins target intracytosolic *Shigella and Listeria* to different autophagy pathways. J Biol Chem 2011;286(30):26987–95.
[41] Abby SS, Cury J, Guglielmini J, Neron B, Touchon M, Rocha EP. Identification of protein secretion systems in bacterial genomes. Sci Rep 2016;6:23080.
[42] Xu Y, Jagannath C, Liu XD, Sharafkhaneh A, Kolodziejska KE, Eissa NT. Toll-like receptor 4 is a sensor for autophagy associated with innate immunity. Immunity 2007;27(1):135–44.
[43] Bonhomme D, Hernandez-Trejo V, Papadopoulos S, Pigache R, Fanton d'Andon M, Outlia A, et al. *Leptospira interrogans* prevents macrophage cell death and pyroptotic IL1ß release through atypical lipopolysaccharide. J Immunol 2023;210:1–16.
[44] Yin S, Cao W. Toll-like receptor signaling induces Nrf2 pathway activation through p62-triggered Keap1 degradation. Mol Cell Biol 2015;35(15):2673–83.
[45] Jiang T, Harder B, Rojo de la Vega M, Wong PK, Chapman E, Zhang DD. p62 links autophagy and Nrf2 signaling. Free Radic Biol Med 2015;88(Pt B):199–204.
[46] Macoch M, Morzadec C, Genard R, Pallardy M, Kerdine-Romer S, Fardel O, et al. Nrf2-dependent repression of interleukin-12 expression in human dendritic cells exposed to inorganic arsenic. Free Radic Biol Med 2015;88(Pt B):381–90.
[47] Helou DG, Braham S, De Chaisemartin L, Granger V, Damien MH, Pallardy M, et al. Nrf2 downregulates zymosan-induced neutrophil activation and modulates migration. PLoS One 2019;14(8):e0216465.
[48] Fanton d'Andon M, Quellard N, Fernandez B, Ratet G, Lacroix-Lamande S, Vandewalle A, et al. *Leptospira Interrogans* induces fibrosis in the mouse kidney through Inos-dependent, TLR- and NLR-independent signaling pathways. PLoS Neglected Trop Dis 2014;8(1):e2664.
[49] Raffray L, Giry C, Vandroux D, Kuli B, Randrianjohany A, Pequin AM, et al. Major neutrophilia observed in acute phase of human leptospirosis is not associated with increased expression of granulocyte cell activation markers. PLoS One 2016;11(11):e0165716.
[50] Gilardini Montani MS, Santarelli R, Granato M, Gonnella R, Torrisi MR, Faggioni A, et al. EBV reduces autophagy, intracellular ROS and mitochondria to impair monocyte survival and differentiation. Autophagy 2019;15(4):652–67.
[51] Bichiou H, Rabhi S, Ben Hamda C, Bouabid C, Belghith M, Piquemal D, et al. *Leishmania* parasites differently regulate antioxidant genes in macrophages derived from resistant and susceptible mice. Front Cell Infect Microbiol 2021;11:748738.
[52] Zavala-Alvarado C, Sismeiro O, Legendre R, Varet H, Bussotti G, Bayram J, et al. The transcriptional response of pathogenic *Leptospira* to peroxide reveals new defenses against infection-related oxidative stress. PLoS Pathog 2020;16(10):e1008904.
[53] Vivarini AC, Calegari-Silva TC, Saliba AM, Boaventura VS, Franca-Costa J, Khouri R, et al. Systems Approach reveals nuclear factor erythroid 2-related factor 2/protein Kinase R crosstalk in human cutaneous Leishmaniasis. Front Immunol 2017;8:1127.